UNIT-II
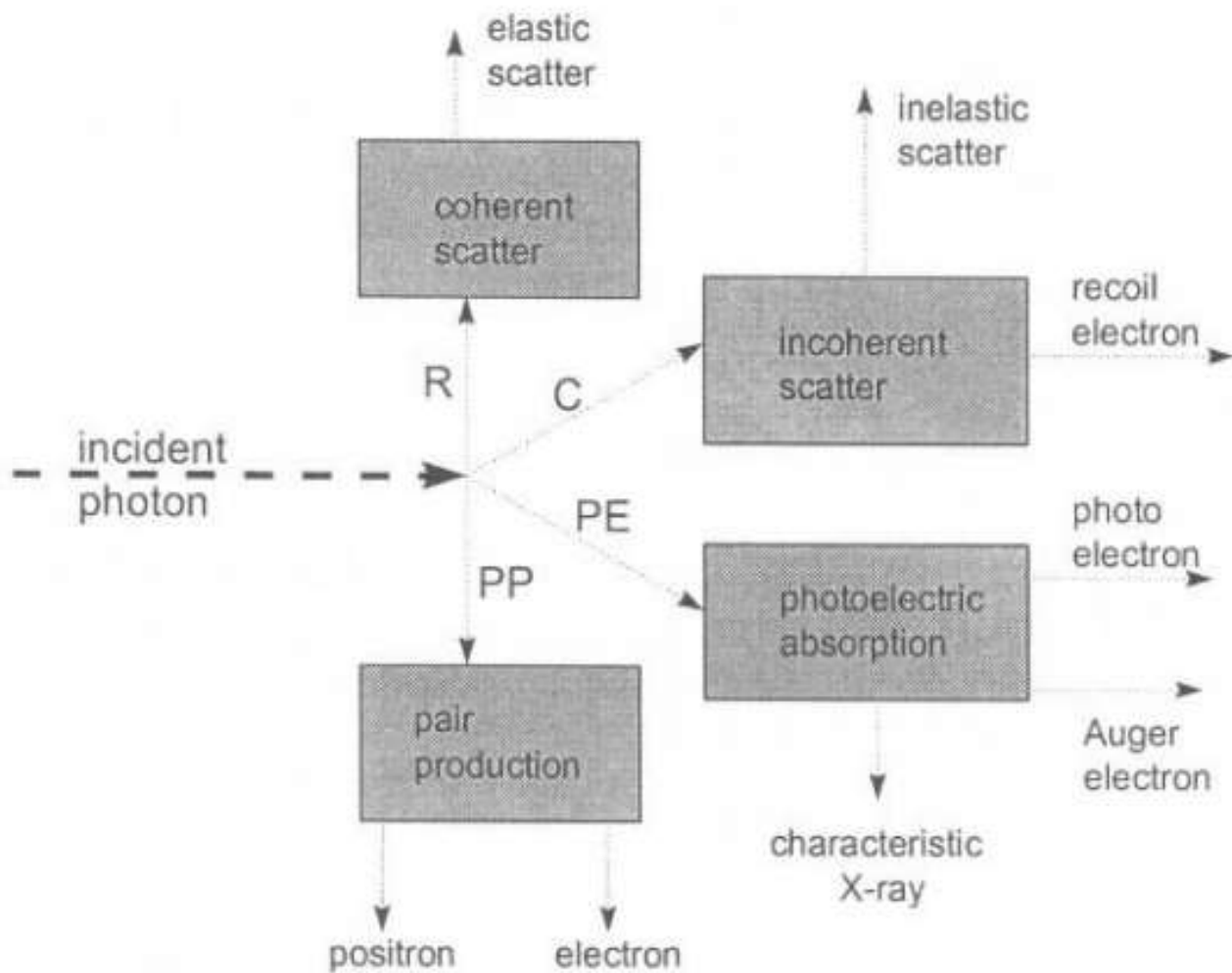## Interaction of Photons (from Smith)

3.1 Introduction

A photon interacts by one of four major processes. The probability of each is determined by a cross-section which depends on the photon energy and on the density and atomic number of the medium.

- Rayleigh (coherent) scatter – the photon interacts with the total electron cloud of an atom.
- Compton (incoherent) scatter – the photon interacts with an individual electron whose binding energy is low compared to that of the incident photon.
- Photoelectric absorption – the photon interacts with an inner atomic electron.
- Pair production – the photon converts into an electron-positron pair when it enters the strong Coulomb field surrounding an atomic nucleus.

Primary photon interaction processes with their secondary emissions.

In addition to the consideration of each individual interaction, it is important to bear in mind the following :

- The attenuation of a beam of photons includes scatter as well as absorption processes. Thus Attenuation = Scatter + Absorption.
- Apart from coherent scatter, all the interaction processes result in the production of electrons. These provide the means by which the major fraction of the photon's energy is imparted to the medium. Consequently, photons are known as indirectly ionizing radiation.
- Secondary photons that emerge from the primary processes – from Rayleigh or Compton scattering of the primary beam or as a characteristic X-ray from a photoelectric absorption – can still undergo any of the four interactions if they are energetically possible.

3.2   Attenuation coefficients (linear, mass, atomic and electronic)

The exponential decrease in the initial number of photons/unit area, Φ_o, which have traversed thickness x of a medium,

$$\Phi = \Phi_o \, exp(-\mu x) \tag{3.1}$$

is expressed in terms of a linear attenuation coefficient, μ. The quantity Φ_0 is called the photon fluence and is considered further in Chapter 7. All of the four processes are included in μ if they are energetically possible.

Fig.(3.2) illustrates the distinction between Good (or narrow) geometry, in which the detection of scattered photons is minimized (position A), and Bad (or wide) geometry, when the effects of scatter are prominent, as in position B. The two cases depend upon :

- the distance between detector and material,
- the size of the detector compared with the width of the beam,
- the energy of the photons,
- the density and mean atomic number of the material.

By definition, the dimension of μ must be reciprocal in length (e.g. cm^{-1}). Its dependence on density is conveniently removed to provide an expression for the mass attenuation coefficients of the individual processes.

$$\frac{\mu}{\rho} = \frac{\sigma_{coh}}{\rho} + \frac{\sigma_{incoh}}{\rho} + \frac{\tau}{\rho} + \frac{\kappa}{\rho} \tag{3.2}$$

detector
position B

detector
position A

The mass attenuation coefficient (μ / ρ) therefore has units $cm^2\ g^{-1}\ (m^2\ kg^{-1})$ when the density is in $g\ cm^{-3}\ (kg\ m^{-3})$. This gives the total attenuation in terms of the individual cross-sections specified per gram (kg) of material.

$$\frac{\sigma_{incoh}}{\rho}\left(cm^2\ g^{-1}\right) = \frac{\sigma_{incoh}}{\rho}\ \frac{A}{ZN_A}\left(cm^2\ electron^{-1}\right)$$

The number of electrons per gram is constant to within ~10% for all materials (apart from hydrogen which has no neutron in its nucleus). This means that the probability of a Compton interaction depends largely on the density of the material and hardly at all on its atomic number.

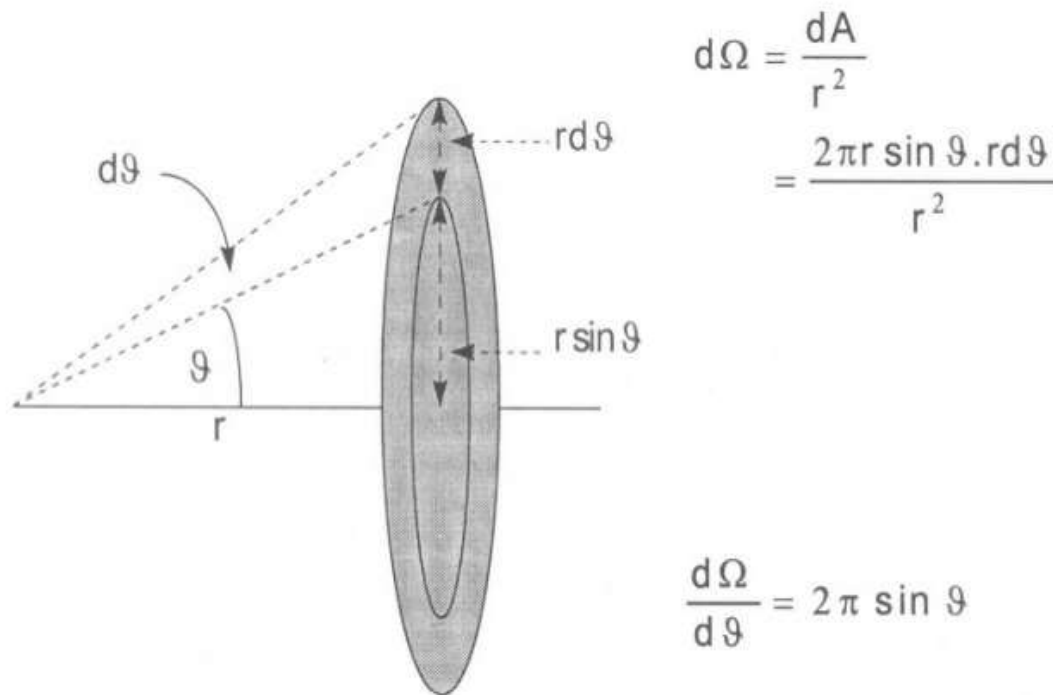### 3.3 Classical (Thomson) scatter from a single electron

$$d\Omega = \frac{dA}{r^2}$$

$$= \frac{2\pi r\ \sin\vartheta \cdot rd\vartheta}{r^2}$$

$$\frac{d\Omega}{d\vartheta} = 2\pi\ \sin\vartheta$$

Fig.(3.3) Relation between ϑ and $d\Omega$ in the scattering of a photon by an electron.

In the classical picture, the incoming electromagnetic wave sets up an electric field at the site of an electron, which is accelerated and which therefore radiates. The probability that the energy contained within the incident wave is scattered into a solid angle $d\Omega$ at an angle of ϑ with respect to the incident direction is called the differential scatter cross-section :

$$\frac{d\sigma_0}{d\Omega} = \frac{r_0^2}{2}\left(1 + \cos^2\vartheta\right) \tag{3.3}$$

where $r_0 = e^2/m_0c^2 = 2.8179 \times 10^{-15}$ m is the classical electron radius. Integration over all angles gives the total cross section σ_0. From Fig.(3.3), we get :

$$\frac{d\sigma_0}{d\vartheta} = \frac{d\sigma_0}{d\Omega}\frac{d\Omega}{d\vartheta} = \frac{r_0^2}{2}\left(1 + \cos^2\vartheta\right)2\pi\sin\vartheta \tag{3.4}$$

The integration of Eq.(3.4) over all angles gives the total Thomson scatter cross-section. This is the area under the ■ symbols in Fig.(3.4) . The result is :

$$\sigma_0 = \frac{8}{3}\pi r_0^2 = 66.53 \times 10^{-30}\, m^2 \,/\, electron \tag{3.5}$$

3.4   Coherent (Rayleigh) scatter

This interaction is due to photon scatter from atomic electrons whose binding energy is considerably greater than the incoming photon energy. The waves interfere constructively to produce a coherent scattered wave. No energy is transferred to the medium (scattered wavelength = incident wavelength) as the Z electrons in the atom take up the recoil momentum without absorbing any energy. Rayleigh scatter becomes more important as the photon energy decreases and the atomic number of the medium increases.

In this case, the Thomson cross-section is multiplied by a form factor, $F(x,Z)$, where Z is the atomic number of the atom, $x = sin(\vartheta/2)/\lambda$, and λ is the wavelength of the photon. $F(x,Z)$ represents the spatial electron distribution in the atom from which the photon can be scattered without any momentum transfer.

$$\frac{d\sigma_{coh}}{d\vartheta} = \frac{r_0^2}{2}\left(1 + cos^2\,\vartheta\right)\left[F(x,Z)\right]^2\, 2\pi\,sin\,\vartheta \tag{3.6}$$

At large angles of scatter, $F(x,Z)$ tends to zero, but the smaller the angle, the more nearly it approximates to Z. This is an atomic cross-section since we are dealing with coherent scatter from all the atomic electrons.

3.5 Incoherent (Compton) scatter

For this interaction the classical theory, which adequately describes low energy photon scatter, has to be replaced by relativistic considerations. This is because the photon energy approaches the rest mass of an electron $m_0c^2 = 511$ keV. The characteristic features of Compton scatter are :

- The momentum of the incident photon is conserved between the outgoing photon and the struck electron.
- Incoherent scattering takes place from individual electrons which, in the majority of cases, appear unbound. When the photon energy becomes comparable with the electron binding energy, it is more probable that photoelectric absorption takes place. However, corrections can be made for Compton scatter from bound electrons using the incoherent scatter function $S(x,Z)$.
- As in all other cases, it is important to distinguish between the probability of an

  interaction taking place and the amount of energy transferred in that process. For a free electron, the former is described by the Klein-Nishina formula, and the latter by the energy and momentum conservation equations.

We consider an incoming photon of energy $E = h\nu_o$ being scattered by an electron,
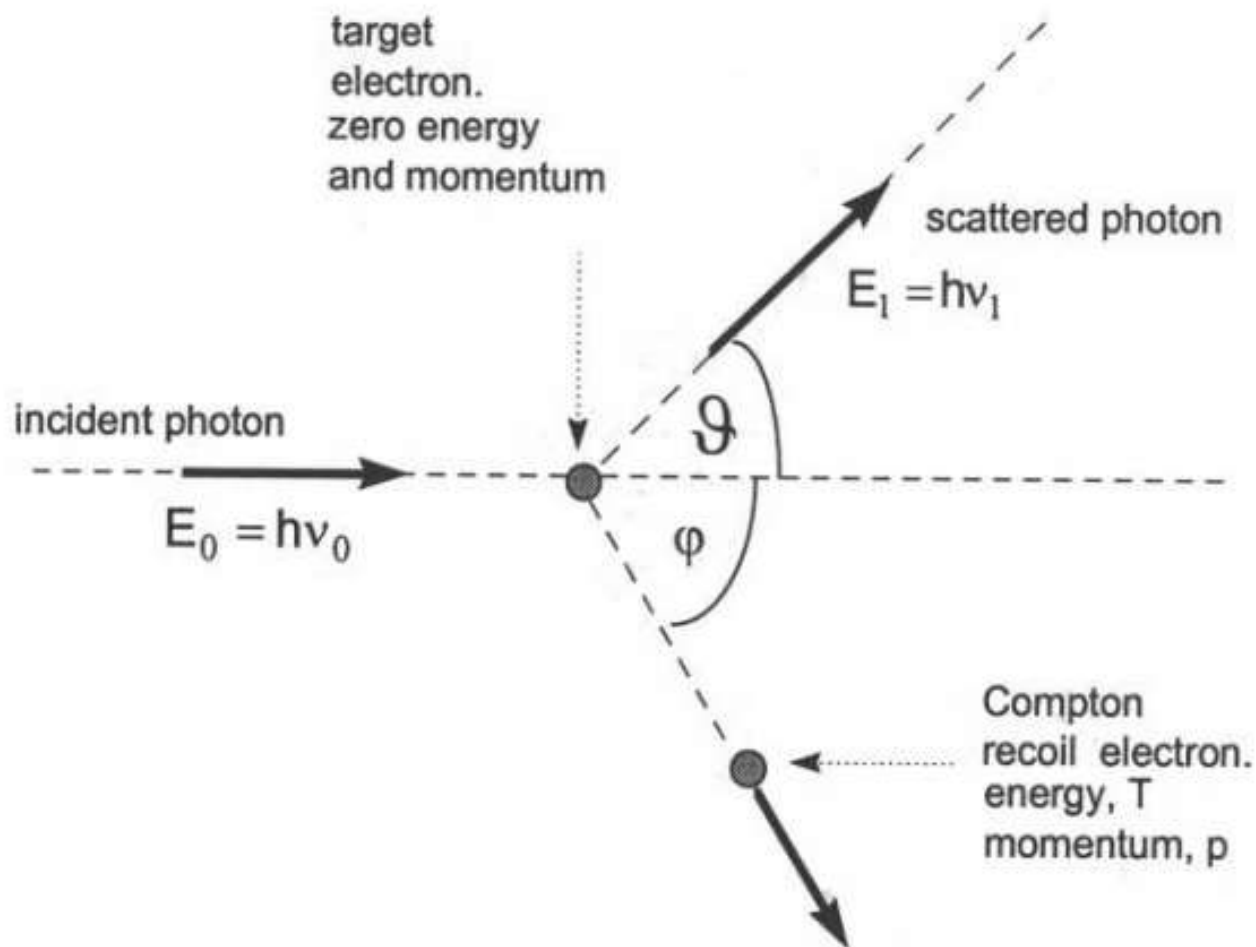[2]. If the electron is not free, its binding energy must be $<< h\nu_o$.

target
electron.
zero energy
and momentum

scattered photon

$E_1 = h\nu_1$

incident photon

$E_0 = h\nu_0$

ϑ

φ

Compton
recoil electron.
energy, T
momentum, p

Fig.(3.7) A schematic diagram of a Compton collision. The incident photon energy is normalized to the electron rest mass using $\alpha = h\nu_o/m_oc^2$.

Energy and momentum are conserved between the electron and photon in Fig.(3.7). Together with the relativistic relation between energy and momentum of the electron we obtain the following equations :

$$h\nu_0 = h\nu_1 + T \qquad (3.8)$$

$$\frac{h\nu_0}{c} = \frac{h\nu_1}{c}\cos\vartheta + p\cos\varphi \qquad (3.9)$$

$$0 = \frac{h\nu_1}{c}\sin\vartheta - p\sin\varphi \qquad (3.10)$$

$$pc = \sqrt{T\left(T + 2m_0c^2\right)} \qquad (3.11)$$

Algebraic manipulation of the above, with $\alpha = h v_0/m_0 c^2$, gives the following relationships :

(a) Compton wavelength shift : $\Delta\lambda = \lambda_1 - \lambda_0 = \dfrac{c}{v_1} - \dfrac{c}{v_0} = \dfrac{h}{m_0 c}(1 - \cos \vartheta)$ (3.12)

The ratio $h/m_0 c$ in Eq.(3.12) is the wavelength of a photon whose energy is just equal to the electron rest mass. It is known as the Compton wavelength, λ_c. Notice that the wavelength shift depends only on scattering angle and not on the incident photon energy.

(b) Energy of scattered photon : $h v_1 = \dfrac{m_0 c^2}{1 - \cos \vartheta + (1 / \alpha)} = \dfrac{h v_0}{1 + \alpha(1 - \cos \vartheta)}$ (3.13)

(c) Energy of the recoil electron : $\qquad T = h v_0 \dfrac{\alpha(1 - \cos \vartheta)}{1 + \alpha(1 - \cos \vartheta)}$ (3.14)

(d) When the collision is head-on and the photon is scattered through 180°, ($\cos\vartheta = -1$), we have the minimum scattered photon energy and the maximum electron recoil energy :

$$T_{max} = h v_0 \dfrac{2\alpha}{1 + 2\alpha}$$

$$h v_{1,min} = h v_0 \dfrac{1}{1 + 2\alpha}$$
  (3.15)

(e) When the collision is grazing (large impact parameter in the notation of section 2.4), then the electron has a minimum energy $T \to 0$ and the photon retains its original energy $h\nu_0$. This takes place when $\vartheta \to 0$, so from Eqs.(3.8) and (3.9), $p \to 0$ and $\varphi \to 90°$.

3.5.1   The Klein-Nishina cross-section for Compton scatter

Having established the kinetics of the collision, we can now consider the probability that the photon is scattered at an angle ϑ with respect to the original direction. This probability is composed of two parts :

- the probability that a collision takes place, i.e. that a photon is removed from the incident beam, $d(_e\sigma)$. The subscript e refers to the fact that we are dealing with scattering from an individual electron.
- the probability that energy is scattered into angle ϑ by the photon, $h\nu_1/h\nu_0$.

The differential cross-section for scatter into angle ϑ is then given by :

$$\frac{d(_e\sigma_s)}{d\Omega} = \frac{h\nu_1}{h\nu_0} \frac{d(_e\sigma)}{d\Omega} \qquad (3.16)$$

The collision probability can be expressed in terms of the angle, η, between the plane containing the scattered photon and the plane containing the electric vector of the incident photon, Fig.(3.8).

$$\frac{d(_e\sigma)}{d\Omega} = \frac{r_0^2}{2}\left(\frac{\nu_1}{\nu_0}\right)^2\left(\frac{\nu_0}{\nu_1} + \frac{\nu_1}{\nu_0} - 2\sin^2\vartheta\cos^2\eta\right) \qquad (3.17)$$

This probability is always largest when $\eta \rightarrow 90°$. It shows that both the photon and the electron tend to emerge at right angles to the electric vector of the incident photon.
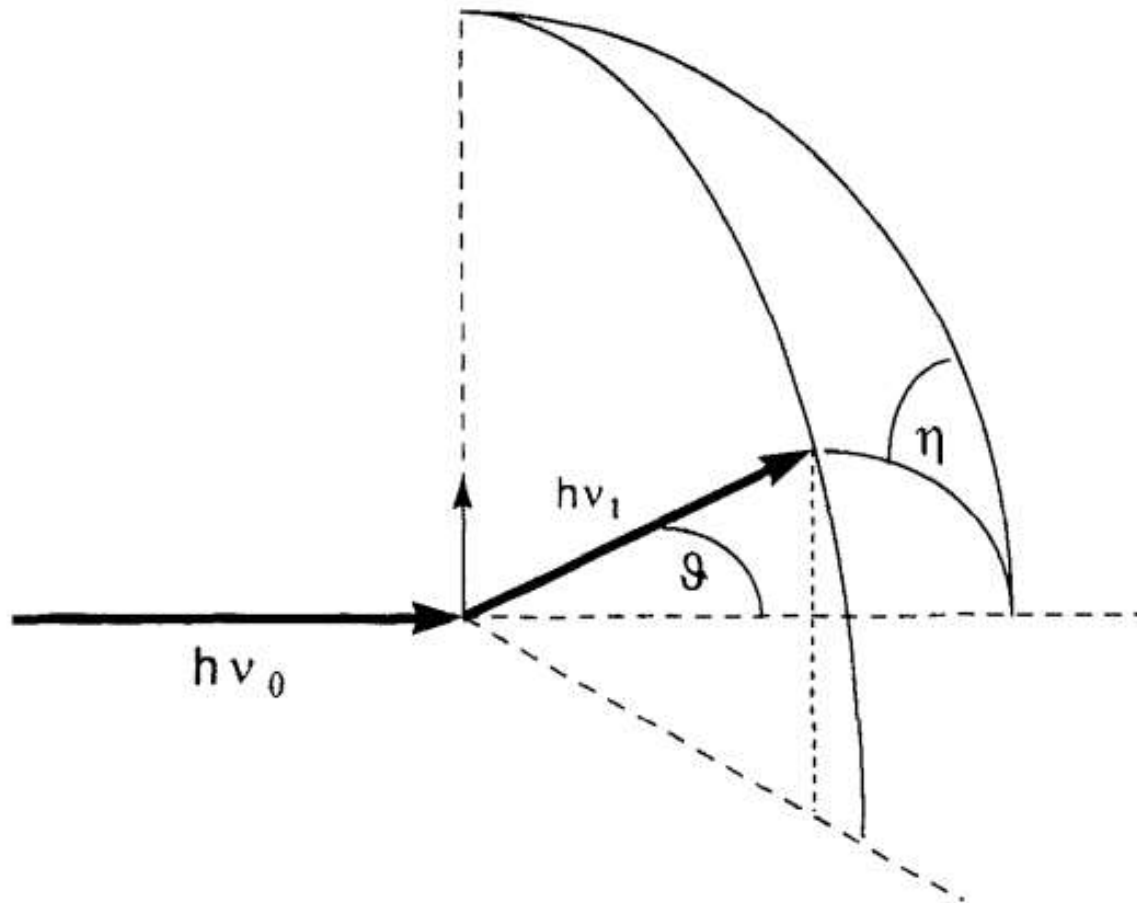
Fig.(3.8) Compton scatter angles for an incident photon polarized with the electric vector in the plane of the paper [2]. With permission from the McGraw Hill Companies.

The differential scattering cross-section for unpolarized radiation can be obtained by summing equal contributions from radiation polarized at right-angles. When the polarization vector is parallel and perpendicular to the plane of the paper in Fig.(3.6), for example, we have $\eta = 0$ and $90°$. Combining Eqs.(3.16) and (3.17) then gives :

$$\frac{d\left(_e\sigma_s\right)}{d\Omega} = \frac{r_0^{\,2}}{2} \left(\frac{h\nu_1}{h\nu_0}\right)^3 \left(\frac{\nu_0}{\nu_1} + \frac{\nu_1}{\nu_0} - \sin^2 \vartheta\right)$$

This can be rewritten in terms of the Thomson scatter cross-section as :

$$\frac{d\left(_e\sigma_s\right)}{d\Omega} = \frac{r_0^{\,2}}{2}\left(1 + \cos^2 \vartheta\right)\left(\frac{1}{1 + \alpha(1 - \cos \vartheta)}\right)^3 \left(1 + \frac{\alpha^2 (1 - \cos \vartheta)^2}{\left(1 + \cos^2 \vartheta\right)\left[1 + \alpha(1 - \cos \vartheta)\right]}\right)$$

(3.18)

Using Eq.(3.3) and a Form Factor, F_{KN}, this is simplified to :

$$\frac{d\left(_e\sigma_s\right)}{d\Omega} = \left(\frac{d\sigma}{d\Omega}\right)_{KN} = \frac{d\sigma_0}{d\Omega} F_{KN}$$

(3.19)

3.5.2 Compton scatter from atomic electrons - the effect of electron binding

The process of photon scatter from an electron or group of electrons involves a momentum change. For a single "unbound" electron – assumed in the Klein-Nishina treatment – the momentum transferred to the electron is related to the recoil energy via Eq.(3.11). If the struck electron has a binding energy which is not negligible compared to the incident photon energy, this momentum is distributed amongst all the electrons in the atom. In a situation where the electrons return to their original states after the interaction, no energy is transferred to the atom and Rayleigh scatter results.

When an electron absorbs some of this momentum, it can be excited into a higher atomic state or emitted from the atom altogether. In either case, the emitted photon has less energy and the scattering is incoherent. This is most likely to occur when the incident photon energy is small and the atomic number is large.

If $q_0 = h\nu_0/c$ and $q_1 = h\nu_1/c$ are the momenta of the incident and scattered photons, Fig.(3.7), the momentum transferred in the collision, Δq, is :

$$(\Delta q)^2 = q_0^2 + q_1^2 - 2q_0 q_1 \cos \vartheta \qquad (3.20)$$

From Eq.(3.13), there is very little change in photon energy when the incident energy is low. In this case, we have $\alpha = h\nu_d/m_oc^2 \to 0$, $h\nu_1 \approx h\nu_o$ and $q_o \approx q_1$. Eq.(3.20) then reduces to :

$$\Delta q \approx \frac{h\nu}{c}\sqrt{2(1 - \cos\vartheta)} = \frac{2h\nu}{c}\sin(\vartheta / 2)$$

The momentum change is therefore just $2h$ times the parameter x used in the atomic form factor $F(x,Z)$.

Not all of the atomic electrons are able to receive the transferred momentum, q, to the same extent. To account for this, an incoherent scatter function, $S(q,Z)$, is defined as:

$$S(q,Z) = Z - \sum_{i=1}^{Z}\left|f_0^i(q)\right|^2 \tag{3.21}$$

In Eq.(3.21), $f_0^i(q)$ expresses the probability that the i' th electron is not excited or detached from the atom, even though it has received recoil momentum q. Thus, if all the electrons are able to participate, the incoherent scatter function is equal to the total number in the atom i.e. the atomic number Z.

The incoherent cross-section in Eq.(3.19) is then corrected for the effects of bound electrons by :

3.5.3　Electron recoil energy in Compton collisions

The energy distribution of recoil electrons is important for two reasons :

- it plays an important role in the energy response of radiation detectors,
- it is important in radiation dosimetry.

The distribution can be obtained from the Klein-Nishina cross-section, Eq.(3.19), together with $d\Omega/d\vartheta$ from Fig.(3.3) and the reciprocal of $dT/d\vartheta$ from Eq.(3.14) :

$$\frac{d\left(_e\sigma_s\right)}{dT} = \frac{d\left(_e\sigma_s\right)}{d\Omega}\frac{d\Omega}{d\vartheta}\frac{d\vartheta}{dT}$$

$$\frac{d\left(_e\sigma_s\right)}{dT} = \frac{3}{8}\sigma_0\frac{1}{\alpha h\nu_0}\left\{1+\cos^2\vartheta+\frac{\alpha^2\left(1-\cos\vartheta\right)^2}{1+\alpha\left(1-\cos\vartheta\right)}\right\}$$
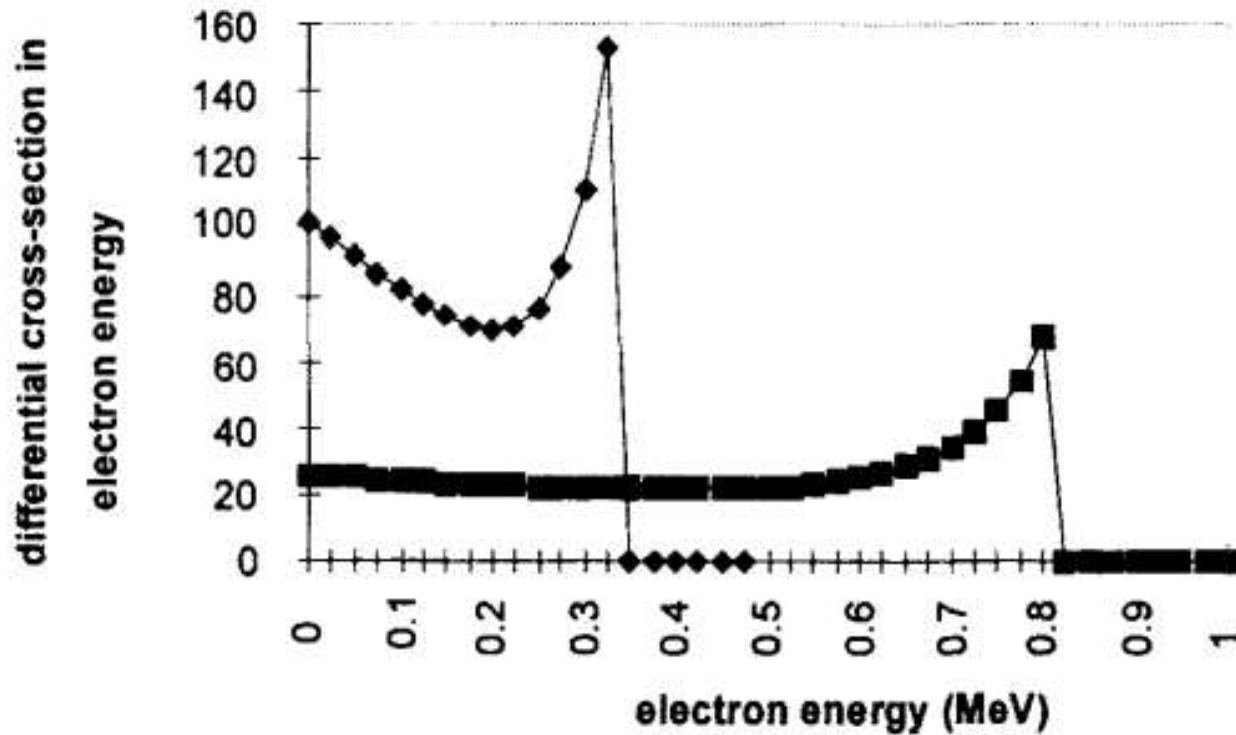
Fig.(3.11)   Compton cross-section differential in electron energy Eq.(3.23) for incident photon energies 0.5 MeV (◆) and 1.0 MeV (■). The ordinate axis is in units of m^2 electron^{-1} MeV^{-1} × 10^{-30}. The maximum electron energies in the two cases are 0.331 MeV and 0.796 MeV respectively, Eq.(3.15). The above curves do not show an infinitely sharp edge (the Compton edge) at these energies because of the finite energy increments taken along the abscissa axis.

The dependence on the scattered photon angle ϑ is eliminated using Eq.(3.14)

to yield the final expression :

$$\frac{d(_e\sigma_s)}{dT} = \frac{3}{8}\frac{\sigma_0}{\alpha h\nu_0}\left\{2 - \frac{2T}{\alpha(h\nu_0 - T)} + \frac{T^2}{\alpha^2(h\nu_0 - T)^2} + \frac{T^2}{h\nu_0(h\nu_0 - T)}\right\} \qquad (3.23)$$

3.5.4 Electron momentum distributions from Compton profiles

Atomic electrons, by virtue of their binding energies, cannot be assumed to be free and stationary. A more complete description should include the initial momentum of the struck electron as well as the polarization vectors of the photon before and after the collision.

A comprehensive review by Cooper [3] refers to an impulsive collision between an incident photon and the free, but moving, electrons. In a collision of this type, the interaction is so rapid that the potential seen by the target electron is the same immediately before, and immediately after, the collision. Conservation of energy can then be stated without the need for any potential energy term, since it cancels from both sides of the equation. This is known as the Impulse Approximation.

Rearrangement of Eq.(3.12) gives the scattered photon energy in terms of the angular frequencies ω_0 and ω_1 :

$$\omega_1 = \frac{\omega_0}{\left[1 + \frac{\omega_0}{m_0 c^2}(1 - \cos\vartheta)\right]} \qquad (3.24)$$

When the scattering vector $\overline{K} = \overline{k}_0 - \overline{k}_1$ is chosen to lie along the z - co-ordinate axis, as in Fig.(3.12), the change in photon energy during the collision is equal to the sum of two terms. The first describes the normal Compton shift expressed in Eqs.(3.13) and (3.24). The second gives the energy associated with the momentum change of the electron along the z-axis. We then have :

$$\omega_0 - \omega_1 = \frac{\hbar^2 |\overline{K}|^2}{2m_0} + \hbar \frac{\overline{K} \cdot \overline{p}_z}{m_0} \qquad (3.25)$$

The energy shift of the photon thereby gives information on the distribution of electron momenta. If the target electrons are described by a probability density distribution, $n(p)$, the projection of this distribution along the z-axis gives the Compton

profile, $J(p_z)$, along the scattering vector as :

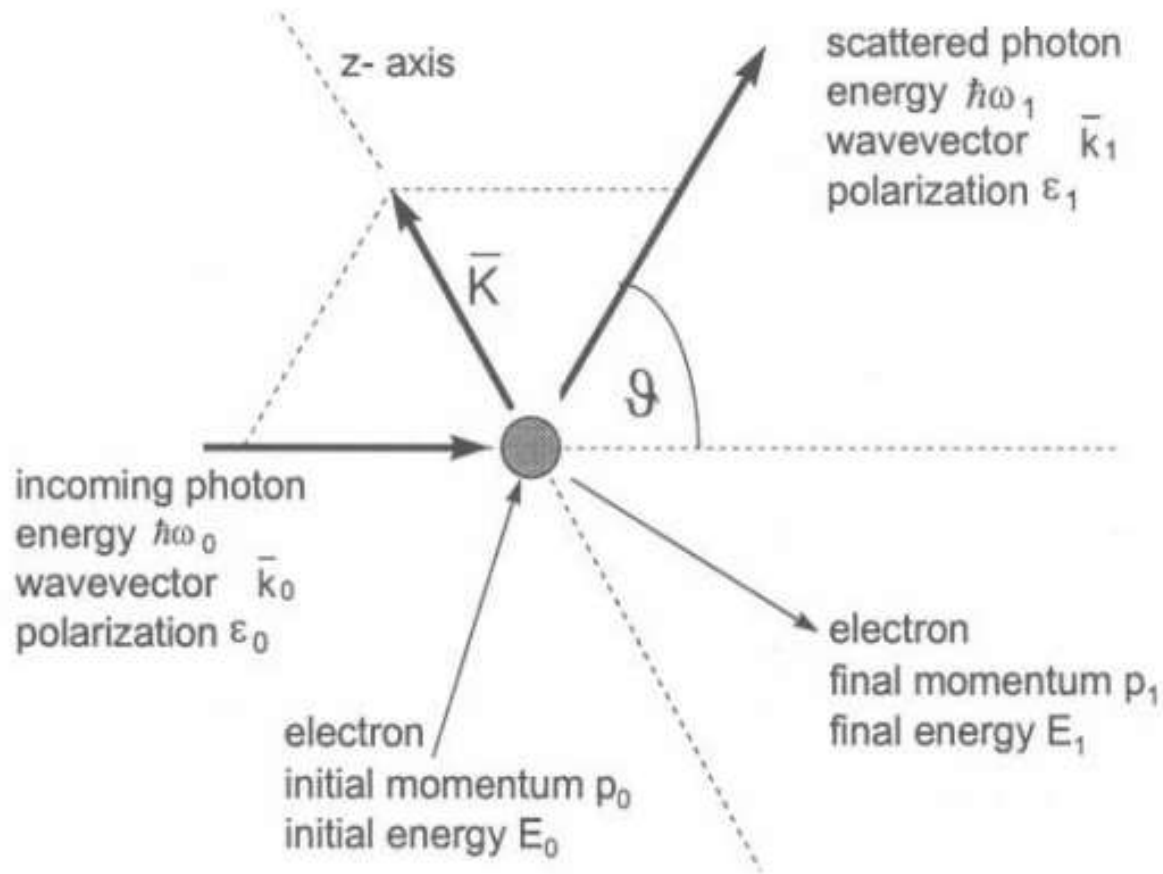$$J(p_z) = \int\limits_{p_x} \int\limits_{p_y} n(p_x, p_y, p_z) dp_x dp_y$$

(3.26)

Fig.(3.12)   The modification of Fig.(3.7) to include the initial and final momenta and energies of the electron, and the polarization vectors of the initial and scatter photon.

At low photon energies ($\hbar\omega_0 \ll m_0 c^2$) the photon energy shift can be related to the momentum of the target electrons by the expression :

$$\omega_0 - \omega_1 = \frac{2\omega_0}{m_0 c} \sin\left(\frac{\vartheta}{2}\right) p_z \tag{3.27}$$

The usefulness of Compton profiling can be illustrated by the application of Eq.(3.27) to a typical situation. Consider a photon scattered through an angle of $180°$ as the result of an interaction with an electron having a component velocity of 2×10^6 m s^{-1} along the scattering vector K. This is the approximate value for an electron at the Fermi surface of aluminium. We have :

$$\sin(\vartheta/2) = 1, \quad p_z/m_0 c = 0.67 \times 10^{-2}, \quad (\omega_0 - \omega_1)/\omega_0 \approx 1.3\%$$

An energy resolution of this magnitude is well within the capability of high purity Ge detectors (Chapter 5). Fig.(3.13) shows the separation of Doppler-shifted photon

energies due to scatter from tightly-bound core electrons and the less tightly-bound conduction electrons in aluminium. The core electron contribution extends to larger energy shifts and signifies photon scatter from higher velocity electrons.
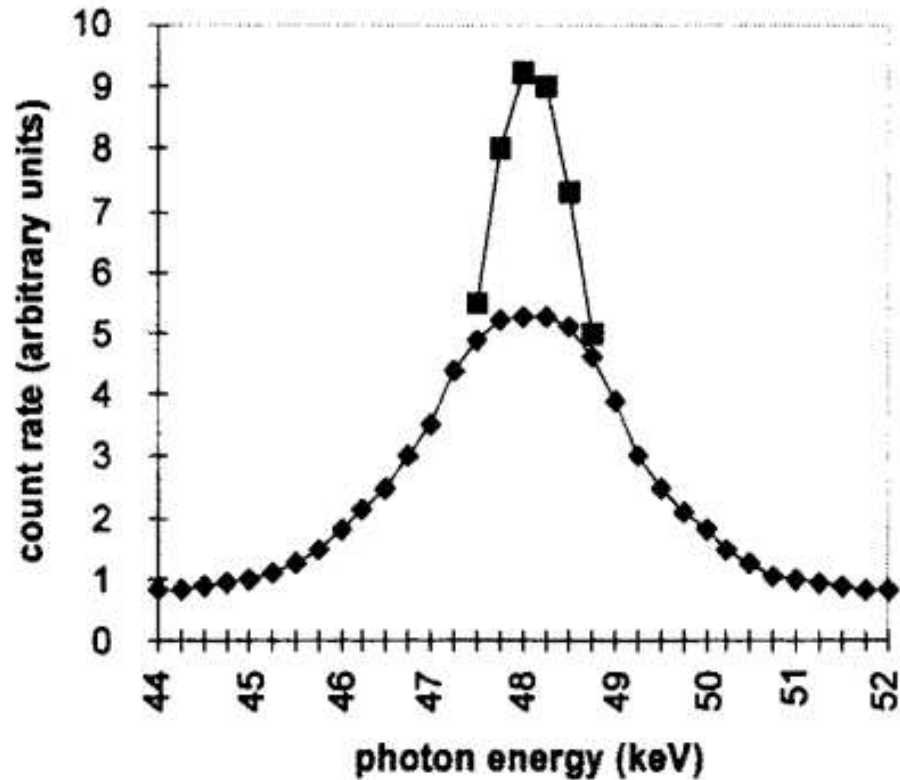

Fig.(3.13) An illustration of a Compton profile using 59.54 keV photons from [241]Am incident on aluminium and scattered at an angle of 171°. Contributions to the total profile come from the 10 core electrons (◆) and the 3 conduction electrons (■) in aluminium, [3].

It is conventional to use atomic units (au) in the determination of electron momenta. These set $e = \hbar = m_0 = 1$ and $c = 137$. The conduction electron component in Fig.(3.13) has a width which extends to ~ 0.8 keV either side of the centroid at $\sim$ 48.2 keV. A maximum conduction electron momentum of $p_z = 0.926$ au is therefore obtained by substituting the following into Eq.(3.27) :

$$\omega_0 - \omega_1 = 0.8 \text{ keV}, \quad \sin(171/2) = 0.997, \quad \omega_0 = 59.54 \text{ keV}, \quad c = 137, \quad m_0 = 1.$$

In the Impulse Approximation, the cross-section is still expressed in terms of the Thomson scatter cross-section, Eq.(3.3), but is now modified to include the Compton profile integral from Eq.(3.26) :

$$\frac{d^2\sigma}{d\Omega d\omega} = \frac{d\sigma_0}{d\Omega} \frac{\omega_1}{\omega_0} \frac{m_0}{|K|} J(p_z) \tag{3.28}$$

Data taken over many scatter angles is then used to determine the Compton profile using Eq.(3.29) to convert between the energy and momentum scales.

$$\frac{p_z}{m_0 c} = \left(\omega_0 - \omega_1\right) \pm \cdot \frac{\omega_0 \omega_1}{m_0 c^2}\left(1 - \cos \vartheta\right)\left(\omega_0^2 + \omega_1^2 - 2\omega_0 \omega_1 \cos \vartheta\right)^{-1/2} \tag{3.29}$$

3.6 Photoelectric Absorption

In this process the photon gives up all its energy in overcoming the binding energy of a bound electron. Any remainder is imparted to the electron as kinetic energy. The photoelectrons so produced from the K, L,…-shells then have kinetic energies:

$$E_K = h\nu_0 - BE_K$$
$$E_L = h\nu_0 - BE_L \tag{3.30}$$

A free electron cannot absorb a photon (and thereby become a photoelectron) because there is no third body to conserve momentum. The tightness of the electron's binding energy increases the ability of the third body (the atom) to absorb the recoil momentum. For this reason, the photoelectric absorption cross-section should be

specified in units of m^2 atom^{-1}. An absorption edge occurs whenever the photon energy reaches an electron binding energy, the discontinuities being greatest for the most tightly bound (K-shell) electrons.

Theoretical computations of the photoelectric cross-section have generally assumed the following :

- the Born approximation. This is based on plane waves for the electron wave function and neglects the attraction of the nuclear charge on the electron as it leaves the atom. Furthermore, this approximation is not valid for incident photon energies comparable to the ionization potential of the atom.
- the initial state is that of a single electron in the central field of the nucleus whose charge is screened by the other electrons.

On this basis Heitler [4] determined the atomic cross-section for K-shell electrons in an atom of atomic number Z as :

$$_a\tau_K = \frac{8}{3}\pi r_0^2 Z^5 \alpha^4 2^{5/2}\left(\frac{m_0 c^2}{h\nu_0}\right)^{7/2} \tag{3.31}$$

In this equation $r_0 = e^2/m_0 c^2$, $\alpha = 2\pi e^2/hc = 1/137$ is the fine structure constant, $m_0 c^2$ is the rest mass of the electron and $h\nu_0$ is the incident photon energy.

A vacancy in a K- (or L-, M-..) shell following photoelectric absorption results in a de-excitation of the atomic system, either by characteristic X-ray or Auger- electron emission. The relative probability of these de-excitation processes is given by the fluorescence yield. For a K-shell vacancy, this is :

$$\omega_K = \frac{P_{KX}}{P_{KX} + P_{KA}}$$

where P_{KX} is the probability of K X-ray emission and P_{KA} is the probability of K Auger emission.

Fluorescence yield is strongly dependent on Z, being small for light atoms and large for heavy atoms. Different semi-empirical relations for the Z-dependence have been proposed. The two most widely quoted are :

$$\omega_K = \frac{Z^4}{a + bZ^4}$$

$$\omega_K = \left(-A + BZ - CZ^3 \right)^4 \tag{3.32}$$

where a, b, A, B, and C are constants. Photoelectric absorption in light atoms is therefore dominated by Auger electron emission, Fig.(3.15).
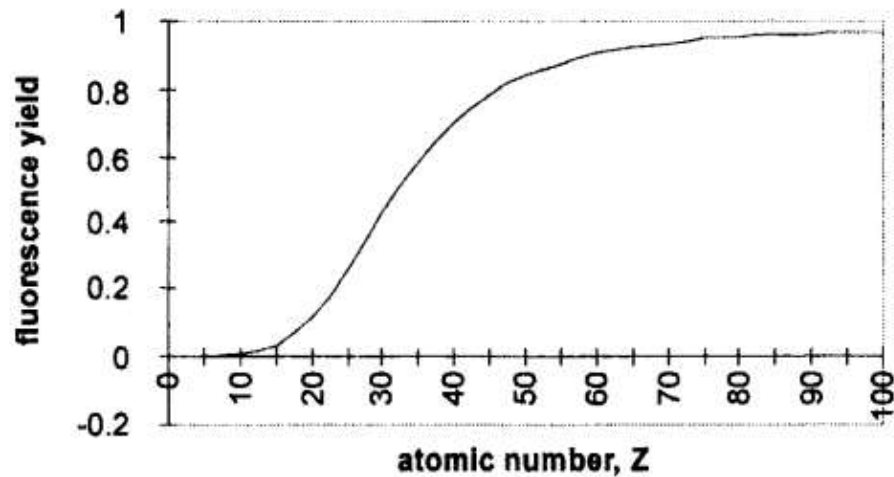
Fig.(3.15)   Fluorescence yield versus atomic number using Eq.(3.32) and constants A=0.064, B=0.034, C=0.00000103.

Auger emission is classified by the atomic energy levels involved. Thus, a vacancy initially created in the K-shell can be filled by an electron from one of the L shells (say L_1). The energy released in this de-excitation process is transferred to another electron in a shell having a smaller binding energy (say L_3). This transition would be designated (K L_1 L_3).

A precise treatment of the emitted electron energies in the Auger effect [6] must consider :

* screening and Coulomb interactions between electrons,
* exchange and spin-orbit interactions.

For practical purposes, however, adequate determinations of Auger electron energies can be obtained from tabulations of sub-shell binding energies [7].

The energy of a (K L$_1$ L$_3$) Auger electron is obtained from Table (3.2) as :

$$2149 - 189 - 135 = 1825 \text{ eV}.$$

In heavy atoms, a special case arises when the transitions take place amongst sub-shells of the same level. These are called Coster-Kronig transitions. Thus, when a primary vacancy in the L level (say L$_1$) is filled by an electron from the L$_3$ sub-shell, the energy difference may be sufficient to expel an electron from a higher shell (say, M$_4$ or M$_5$).

For tungsten, Table (3.2) shows that the Coster-Kronig electron energies in each of these cases are :

$$(L_1 \ L_3 \ M_4) = 12099 - 10205 - 1872 = 22 \text{ eV}.$$
$$(L_1 \ L_3 \ M_5) = 12099 - 10205 - 1810 = 84 \text{ eV}.$$

Table (3.2) Sub-shell electron binding energies (eV) in phosphorous and tungsten, [7].

	K	L1	L2	L3	M1	M2	M3	M4	M5
P (Z=15)	2149	189	136	135	16	10	-	-	-
W (Z=74)	69525	12099	11542	10205	2820	2575	2281	1872	1810

3.7 Pair Production

In contrast to the main energy dependence of Rayleigh, Compton and photoelectric interaction processes, the probability of pair production increases with increasing photon energy. It takes place in the field of a charged particle – mostly in the strong Coulomb field of the nucleus, although it can also take place at high energies in the field of an electron.

Pair production has a threshold photon energy equal to the combined rest mass of two electrons. Thus :

$$hv = (T^+ + m_0 c^2) + (T^- + m_0 c^2)$$

As in the case of photoelectric absorption, the interaction is treated initially on the basis of the Born approximation [8]. Here the assumption is that :

- Ze^2/hv <<1. Such a treatment is therefore not valid for large Z or small photon (and hence positron or electron) energies.
- When the interaction takes place close to the nucleus, pair production takes

place in the Coulomb field of the nucleus. At larger distances, this field is screened by the orbiting electrons by an amount which depends on distance from the nucleus. The part played by these electrons is assumed only to affect the screening of the nuclear charge and not to affect the dynamics of the collision.
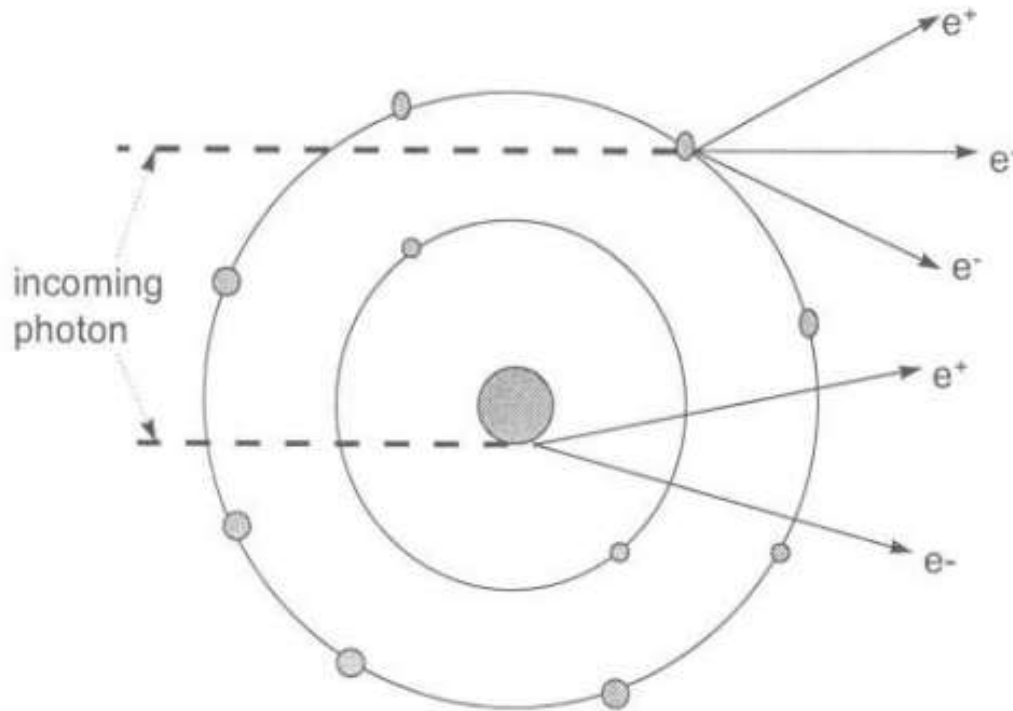- The emitted electrons are represented by plane waves.

Fig.(3.16)   Representation of pair production close to the nucleus (threshold energy 1.02 MeV) and triplet production far from the nucleus (threshold energy 2.04 MeV), [9]. With permission from Charles C. Thomas Ltd., Springfield, Illinois.

$$_a\kappa = \frac{1}{137}r_0{}^2 Z^2\left(\frac{28}{9}\ln\left(\frac{2h\nu}{m_0 c^2}\right) - \frac{218}{27}\right) \tag{3.33}$$

where $r_0 = e^2/m_0 c^2$ = classical electron radius = 2.818×10^{-15}m. The constant factor $r_0{}^2/137$ is equal to 5.80×10^{-32} m^2 nucleus^{-1}.

A result for triplet production due to [10] gives :

$$_a\kappa_{triplet} = \frac{1}{137}r_0{}^2 Z\, \frac{\pi\sqrt{3}}{972}\left(\frac{h\nu - 4m_0 c^2}{m_0 c^2}\right)^2 \tag{3.34}$$

Note that Eqs.(3.33) and (3.34) give the cross-sections in m^2/nucleus and show a Z^2 (pair) and Z (triplet) dependence respectively.